General details

The synthesis and characterisation of DFO-ArN_3 was reported elsewhere.(*1*) Unless otherwise stated, all chemicals were of reagent grade and purchased from SigmaAldrich (St. Louis, MO), Merck (Darmstadt, Germany), Tokyo Chemical Industry (Eschborn, Germany), abcr (Karlsruhe, Germany) or CheMatech (Dijon, France). Water (>18.2 MΩ·cm at 25 ºC, Puranity TU 3 UV/UF, VWR International, Leuven, Belgium) was further purified by using Chelex resin to remove contaminant metal ions. Solvents for reactions were of reagent grade, and where necessary, were dried over molecular sieves. Evaporation of the solvents was performed under reduced pressure by using a rotary evaporator (Rotavapor R-300, Büchi Labortechnik AG, Flawil, Switzerland) at the specified temperature and pressure. Electronic absorption spectra were recorded using a Nanodrop^{TM} One^{C} Microvolume UV-Vis Spectrophotometer (ThermoFisher Scientific, supplied by Witec AG, Sursee, Switzerland). Protein concentration was determined in accordance with the manufacturers protocol.

Photochemistry

Photochemical conjugation experiments were performed in transparent glass vials at the specified concentrations. Unless otherwise stated, photochemical reactions were typically stirred gently by adding a small magnetic stir bar to the reaction vial and employing a slow stirring rate (< 1000 rpm) to avoid potential damage to the protein. Detail procedures and reaction times are indicated in the experimental section. Ultra-violet irradiations were performed by using a portable light-emitting diode (LED 365 nm). The LED intensity was adjusted using a digital UV-LED controller (Opsytec Dr. Gröbel GmbH, Ettlingen, Germany), where 100% corresponded to a power of approximately 263 mW at 365 nm. LED intensity was measured by using a S470C Thermal Power Sensor Head Volume Absorber, 0.25 – 10.6 µm, 0.1 mW – 5W, Ø15 mm. The temperature of all photochemical conjugation reactions was typically 23 ± 2 ºC (ambient conditions). An experimentally measured emission spectrum of the LED light source and a plot of the power *versus* digitally controlled LED intensity (as a percentage of maximum current) are shown in Supplemental Figures 1A and 1B, respectively. The LED source (365 nm) had a linear response with changing LED intensity with a peak emission at 364.5 nm and a FWHM of 9.1 nm.

Supplemental Figure 1. (A) Emission spectrum of the LED (365 nm), and (B) the measured power output (mW) *versus* the digitally controlled LED intensity (%).

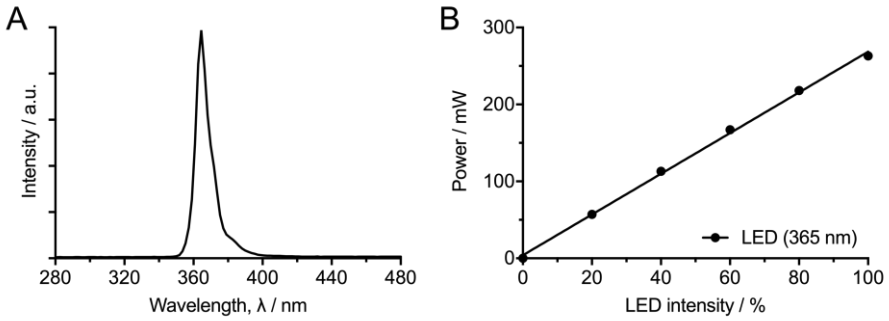

Radioactivity and radioactive measurements

All instruments for measuring radioactivity were calibrated and maintained in accordance with previously reported routine quality control procedures.(*2*) $[^{89}Zr][Zr(C_2O_4)_4]^{4-}$(aq.) was obtained as a solution in ~1.0 M oxalic acid from PerkinElmer (Boston, MA, manufactured by the BV Cyclotron VU, Amsterdam, The Netherlands) and was used without further purification. Radioactive reactions were monitored by using instant thin-layer chromatography (radio-iTLC). Glass-fibre iTLC plates impregnated with silica-gel (iTLC-SG, Agilent Technologies) were developed in using aqueous mobile phases containing DTPA (50 mM, pH7.1) and were analysed on a radio-TLC detector (SCAN-RAM, LabLogic Systems Ltd, Sheffield, United Kingdom). Radiochemical conversion (RCC) was determined by integrating the data obtained by the radio-TLC plate reader and determining both the percentage of radiolabelled product (R_f = 0.0) and 'free' ^{89}Zr (R_f = 1.0; present in the analyses as $[^{89}Zr][Zr(DTPA)]^-$). Integration and data analysis were performed by using the software Laura version 5.0.4.29 (LabLogic). Appropriate background and decay corrections were applied as necessary. Radiochemical purities (RCPs) of labelled protein samples were determined by size-exclusion chromatography (SEC) using two different columns and techniques. The first technique used an automated size-exclusion column (Bio-Rad Laboratories, ENrich SEC 70, 10 ± 2 µm, 10 mm ID x 300 mm) connected to a Rigol HPLC system (Contrec AG, Dietikon, Switzerland) equipped with a UV/visible detector (absorption measured at 220, 254 and 280 nm) as well as a radioactivity detector (FlowStar^2 LB 514, Berthold Technologies, Zug, Switzerland). Isocratic elution with phosphate buffered saline

(PBS, pH7.4) was used. The second method used a manual procedure involving size-exclusion column chromatography and a PD-10 desalting column (Sephadex G-25 resin, 85-260 µm, 14.5 mm ID x 50 mm, >30 kDa, GE Healthcare). For analytical procedures, PD-10 columns were eluted with PBS. A total of 40 x 200 µL fractions were collected up to a final elution volume of 8 mL. Note that the loading/dead-volume of the PD-10 columns is precisely 2.50 mL which was discarded prior to aliquot collection. For quantification of radioactivity, each fraction was measured on a gamma counter (HIDEX Automatic Gamma Counter, Hidex AMG, Turku, Finland) using an energy window between 480 – 558 keV for ^{89}Zr (511 keV emission) and a counting time of 30 s. Appropriate background and decay corrections were applied throughout. PD-10 SEC columns were also used for preparative purification and reformulation of radiolabelled products (in sterile PBS; pH7.4) by collecting a fraction of the eluate corresponding to the high molecular weight protein (>30 kDa fraction eluted in the range 0.0 mL to either 1.6 mL or 1.8 mL as indicated for each experiment).

Synthesis and chemical characterisation

Chemical synthesis and characterisation of DFO-ArN_3 and DFO-Bn-NCS-onartuzumab were performed in accordance with previously reported methods.(*1*,*3*) Note, the bioconjugation reaction using DFO-Bn-NCS,(*4*)(*5*) required pre-purification of the humanized, monovalent onartuzumab protein from the formulated solution of MetMAb by standard spin centrifugation methods.

^{89}Zr-radioactive stocks

A stock solution of [^{89}Zr][Zr(C_2O_4)$_4$]$^{4-}$ was prepared by adding ^{89}Zr radioactivity from the source (222.7 MBq, 140 µL in ~1.0 M aqueous oxalic acid) to an Eppendorf tube. The solution was neutralised and made slightly basic by the addition of aliquots of Na_2CO_3(aq.) (1.0 M stock solution, total volume of 180 µL added, final pH ~8.3 – 8.5, final volume ~320 µL, final activity = 215.8 MBq). Caution: Acid neutralisation with Na_2CO_3 releases CO_2(g) and care should be taken to ensure that no radioactivity escapes the microcentrifuge tube. After CO_2 evolution ceased, different reactions were performed at the same time using the same stock solutions.

Radiochemistry

Simultaneous photoradiosynthesis of [^{89}Zr]ZrDFO-azepin-onartuzumab

Simultaneous, one-pot photochemical conjugation and ^{89}Zr-radiolabelling reactions were performed in accordance with the following general procedure. A stock solution of DFO-ArN_3 was prepared by dissolving the purified white solid (**1**, 0.69 mg, 0.978 μmol) in H_2O (950 μL) and NaOH(aq.) (60 μL of a 0.1 M stock solution). The pH of the DFO-ArN_3 solution was adjusted to ~8 – 9 by the addition of HCl(aq.) (40 μL of a 0.1 M stock solution) and the final concentration of compound **1** was 0.932 mM. Note: DFO-ArN_3 (**1**) is sparingly soluble at high pH and starts to precipitate slowly when the pH decreases below ~9. Reactions were performed in optically transparent and colourless 2 mL glass vials equipped with small magnetic stirring bars.

Photoradiosynthesis of [^{89}Zr]ZrDFO-azepin-onartuzumab for animal experiments

To a glass vial containing H_2O (30 μL; chelex treated 18.2 MΩ.cm) was added an aliquot of the DFO-ArN_3 (**1**) stock solution (40 μL, 37.3 nmol). Then an aliquot of the neutralised stock solution of [^{89}Zr][Zr(C_2O_4)$_4$]$^{4-}$ was added (70 μL, 45.2 MBq). Then an aliquot of the stock solution of MetMAb was added (fully formulated, stock concentration = 60 mg/mL, MW(onartuzumab) = 99,180 Da, volume added = 10 μL, protein mass = 0.6 mg, protein moles = 6.05 nmol). The initial chelate-to-mAb ratio was 6.15 to 1. The reaction pH was measured and was between 7.9 – 8.3. The total reaction volume was ~150 μL giving a final [mAb] = 40.3 μM, and a final [DFO-ArN_3] = 248 μM. The reaction was stirred gently at room temperature and irradiated directly from the top of the vial for 10 min. Previous experiments using this reaction geometry confirmed that this was sufficient to affect ~100% photochemical reaction of the aryl azide group on compound **1**.(*1*) After the irradiation, reactions were then quenched by the addition of DTPA (10 μL, 50 mM, pH7) and aliquots of the crude reaction mixtures were purified by preparative PD-10-SEC (collecting the 0.0 – 1.6 mL high molecular weight fraction using sterile PBS as an eluent). Crude and pure mixtures were analysed by using analytical radio-ITLC, PD-10-SEC and SEC-HPLC. The isolated decay corrected radiochemical yield (RCY) of [^{89}Zr]ZrDFO-azepin-onartuzumab was 24.8% (n = 1) and the lower limit of the molar activity of

the product (estimated by assuming no protein losses) was ~1.5 MBq/nmol of protein, with an activity concentration of 3.87 MBq/mL. The radiochemical purity of the purified samples of [^{89}Zr]ZrDFO-azepin-onartuzumab was estimated to be ~90% (measured by SEC-HPLC).

Preparation of [^{89}Zr]ZrDFO-azepin-onartuzumab doses for injection

An aliquot of (2.463 MBq) of the purified and formulated sample of [^{89}Zr]ZrDFO-azepin-onartuzumab was added to a sterile vial and diluted with sterile PBS to a final volume of 1.1 mL. Syringes containing an average of 222 ± 15 µL were drawn with the average dose containing 0.471 ± 0.047 MBq (equivalent to 30.3 ± 0.31 µg of protein, 0.336 ± 0.031 nmol of protein).

For the competitive inhibition (blocking) experiments, a separate aliquot (2.410 MBq) of the purified and formulated sample of [^{89}Zr]ZrDFO-azepin-onartuzumab was added to a sterile vial. Then an aliquot of the stock solution of MetMAb (fully formulated; 60 mg/mL, 83 µL, 4.98 mg of protein) was added and the mixture was diluted with sterile PBS to a final volume of 1.1 mL. Syringes containing an average of ~208 ± 3 µL were drawn with the average dose containing 0.433 ± 0.011 MBq (equivalent to 971 ± 14 µg of protein, 9.79 ± 0.144 nmol of protein – a 29-fold increase in the administered protein mass for these blocking doses compared to the normal doses).

Classical radiosynthesis of [^{89}Zr]ZrDFO-Bn-NCS-onartuzumab

Radiosynthesis of [^{89}Zr]ZrDFO-Bn-NCS-onartuzumab for animal experiments

Conjugated DFO-Bn-NCS-onartuzumab was prepared as previously reported(*3*) using the standard protocol from Vosjan *et al*.(*4*) Radiolabelling with [^{89}Zr][Zr(C_2O_4)$_4$]$^{4-}$ was accomplished by using standard procedures.(*6*) Briefly, an aliquot of DFO-Bn-NCS-onartuzumab (65 µL formulated in saline, stock protein concentration = 3.84 mg/mL, pH7, protein mass = 0.250 mg, protein moles = 2.52 nmol) was added to an Eppendorf tube containing water (107 µL; chelex treated 18.2 MΩ.cm). Then an aliquot of the neutralised stock solution of [^{89}Zr][Zr(C_2O_4)$_4$]$^{4-}$ was added (60 µL, 39.4 MBq,). The reaction pH was measured and was between 7.9 – 8.3. The total reaction volume was ~232 µL giving a final [mAb] = 10.9 µM. The reaction was incubated at room temperature for ~45 min. and was then quenched by the addition of DTPA (10 µL, 50 mM, pH7). Aliquots of the crude reaction mixtures were purified by

preparative PD-10-SEC (collecting the 0.0 – 1.6 mL high molecular weight fraction using sterile PBS as an eluent). Crude and pure mixtures were analysed by using analytical radio-ITLC, PD-10-SEC and SEC-HPLC. The isolated decay corrected radiochemical yield (RCY) of [^{89}Zr]ZrDFO-azepin-onartuzumab was >97% (n = 1) and the lower limit of the molar activity of the product (estimated by assuming no protein losses) was ~14.0 MBq/nmol of protein, with an activity concentration of 19.0 MBq/mL. The radiochemical purity of the purified samples of [^{89}Zr]ZrDFO-azepin-onartuzumab was estimated to be >97% (measured by SEC-HPLC).

Preparation of [^{89}Zr]ZrDFO-Bn-NCS-onartuzumab doses for injection

An aliquot of (2.463 MBq) of the purified and formulated sample of [^{89}Zr]ZrDFO-Bn-NCS-onartuzumab was added to a sterile vial and diluted with sterile PBS to a final volume of 1.1 mL. Syringes containing an average of 210 ± 2 µL were drawn with the average dose containing 0.571 ± 0.016 MBq (equivalent to 4.04 ± 0.15 µg of protein, 0.041 ± 0.001 nmol of protein).

Supplemental Figure 2. Radio-iTLC chromatograms recorded during the production of [^{89}Zr]ZrDFO-Bn-NCS-onartuzumab and [^{89}Zr]ZrDFO-azepin-onartuzumab for use in animal studies.

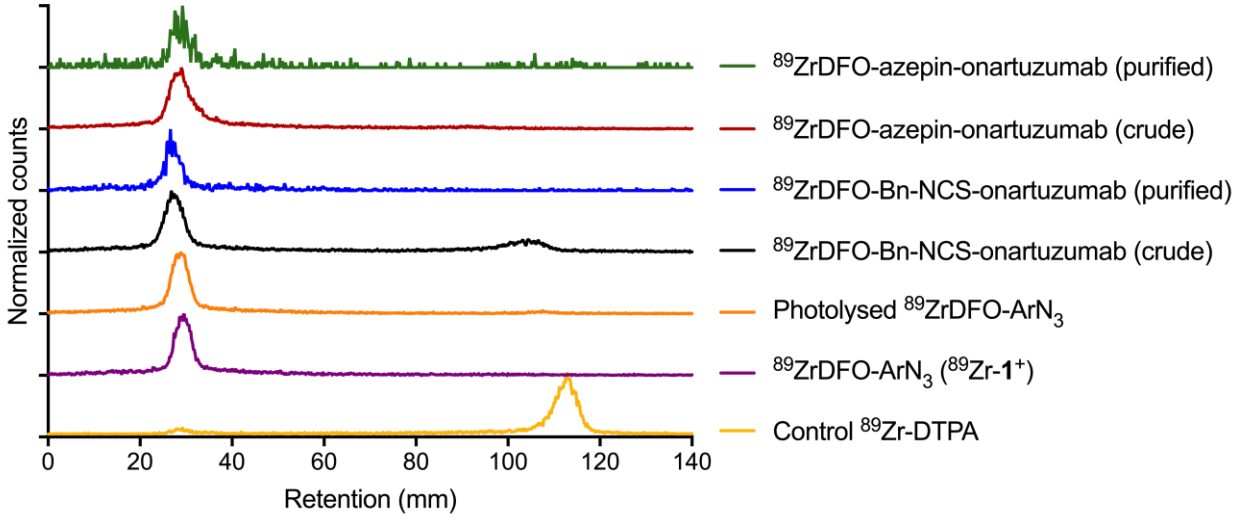

Optimisation of the photoradiosynthesis of [^{89}Zr]ZrDFO-azepin-onartuzumab

Effect of changing the initial chelate-to-mAb ratio and protein concentration

Experiments were performed to measure the effect of altering the initial chelate-to-mAb ratio on the efficiency of the simultaneous, one-pot photochemical conjugation and ^{89}Zr-radiolabelling of onartuzumab (using fully formulated MetMAb). Photoradiosynthesis experiments were set-up in an identical fashion to the reaction used to produce the dose for use in animal experiments. Unless otherwise stated, all reactions were stirred gently and were performed in triplicate using independent replicates. In all cases, the final reaction volume was 160 µL. All reactions were irradiated using 365 nm light for 10 min at ambient temperature. The protein concentration of the stock solution of formulated MetMAb was 60 mg/mL. The [DFO-ArN_3] was 0.932 mM. The same neutralised stock solution of [^{89}Zr][Zr(C_2O_4)$_4$]$^{4-}$ was used throughout and all experiments were performed on the same day to limit the effects of changes in molar activity. Full details are given in Supplemental Table 1.

Supplemental Table 1. Reaction parameters used during the optimisation of the one-pot photoradiosynthesis of [^{89}Zr]ZrDFO-azepin-onartuzumab starting from formulated MetMAb.

Parameter	Reactions A, B and C	Reactions D, E and F	Reactions G, H and I	Reaction J (not stirred)[b]	Reactions K and L	Reactions M and N	Reactions O and P	Reactions Q and R
Vol. MetMAb stock / µL	10	10	10	10	3.2	1	0.32	0.1
n(mAb) / nmol	6.05	6.05	6.05	6.05	1.91	0.605	0.19	0.06
Vol. DFO-ArN_3 stock / µL	30	15	5	30	30	30	30	30
n(DFO-ArN_3) / nmol	27.95	13.97	4.66	27.95	27.95	27.95	27.95	27.95
Initial chelate-to-mAb ratio	4.62	2.31	0.77	4.62	14.6	46.2	146.1	461.9
Radiochemical conversion (RCC) / % measured from SEC-HPLC for each replicate	A = 57.1 B = 61.9 C = 51.9	D = 63.8 E = 56.0 F = 58.2	G = 59.6 H = 56.1 I = 59.5	J = 56.5	K = 23.6 L = 25.6	M = 27.5 N = 18.7	O = 6.7 P = 5.6	Q = 13.7 R = 8.6
Average RCC ± one standard deviation (s.d.) / %	56.9 ± 4.1	59.3 ± 3.3	58.4 ± 1.6	56.5	24.6 ± 1.4	23.1 ± 6.2	6.1 ± 0.8	11.1 ± 3.6
Isolated decay corrected radiochemical yield (RCY) / %[a]	41.2 ± 10.6	33.7 ± 5.8	34.9 ± 10.4	Not determined	Not determined	Not determined	Not determined	Not determined
Average radiochemical purity (RCP) /% of the purified samples measured by SEC-HPLC	91.6 ± 0.6	91.3 ± 1.8	90.7 ± 2.3	Not determined	Not determined	Not determined	Not determined	Not determined

[a] RCY determined after isolation using preparative PD-10 SEC. [b] n = 1 replicate.

Stability studies

The stability of [^{89}Zr]ZrDFO-azepin-onartuzumab and [^{89}Zr]ZrDFO-Bn-NCS-onartuzumab with respect to change in radiochemical purity due to loss of radioactivity from the protein fraction was investigated *in vitro* by incubation in human serum. Aliquots (80 µL) of the purified and formulated radiotracers were added to a solution of human serum (320 µL) giving a total reaction volume of 400 µL. Solutions were incubated at 37 ºC and samples were withdrawn at various time points up to 48 h for analysis by SEC-HPLC measurements. The stability was monitored by quantifying the radioactivity associated with intact [^{89}Zr]ZrDFO-azepin-onartuzumab from integration of the decay corrected and baseline corrected SEC-HPLC radioactive chromatograms.

Supplemental Figure 3. Radioactive SEC-HPLC chromatograms recorded from samples [^{89}Zr]ZrDFO-Bn-NCS-onartuzumab (blue) and [^{89}Zr]ZrDFO-azepin-onartuzumab (green) incubated in human serum at 37 ºC for up to 48 h.

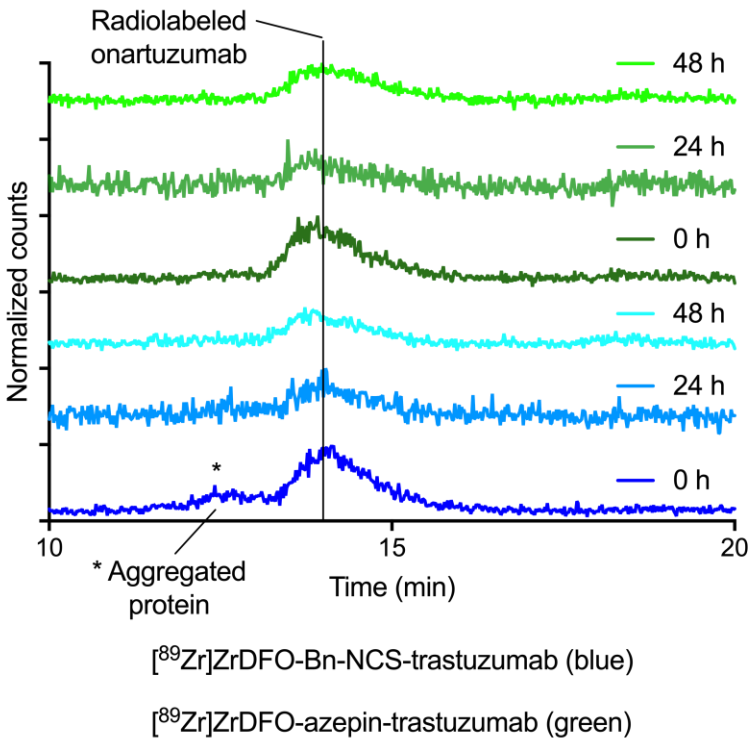

Cell culture

For cell binding assays, the human gastric cancer cell line MKN-45 (c-MET positive and overexpressing, Leibniz Institute DSMZ-German collection of Microorganisms and Cell cultures [ACC 409]) was used. Cells were cultured at 37 °C in a humidified 5% CO_2 atmosphere. MKN-45 cells were cultured in RPMI-1640 (without phenol-red). The media was supplemented with fetal bovine serum (FBS, 10% (v/v), ThermoFisher Scientific) and penicillin/streptomycin (P/S, 1% (v/v) of penicillin 10000 U/mL and streptomycin 10 mg/mL). Cells were grown by serial passage and were harvested using trypsin-EDTA solution (0.025%). Cells were pelleted (100 g, 5 min) and resuspended in media before sequential passaging.

Cell binding assays (immunoreactivity)

Immunoreactivity was determined using a procedure adapted from Lindmo *et al*.(*7*) Briefly, MKN-45 cells were harvested and collected by centrifugation (100 g, 5 min). Two concentration series of 1:2 dilutions (in triplicate) were prepared in RPMI media. To one series, aliquots of purified [^{89}Zr]ZrDFO-azepin-MetMAb (~ 5 ng, ~ 335 Bq, 100 μL PBS) were added, and to the other, aliquots of purified [^{89}Zr]ZrDFO-Bn-NCS-MetMAb (~ 5 ng, ~ 3442 Bq, 100 μL PBS) were added to each cell concentration. To determine the extent of non-specific binding a fourth concentration series of the highest three concentrations was prepared and an ~35,000-fold excess of non-functionalised MetMAb (3 μL, 60 mg/mL, 0.18 mg) was added 30 min. before the addition of the radiotracer. Three samples of control radiotracers were also prepared to serve as standards for total activity added in the vials for each series. Vials were shaken gently at 400 rpm at 37 °C in a thermomixer for 4 h to ensure the cells remained in suspension. The cells were then pelleted by centrifugation (2000 rpm, 4 °C, 4 min.), the media was removed and the cells were washed twice with ice cold PBS with re-pelleting and removal of PBS between each wash. Cell associated radioactivity of the washed pellet was measured by using a Hidex gamma counter. The immunoreactive fraction was determined as the reciprocal y-intercept from the Lindmo transformation.

Supplemental Figure 4. Measurement of the immunoreactive fraction of [^{89}Zr]ZrDFO-azepin-onartuzumab (blue) and [^{89}Zr]ZrDFO-Bn-NCS-onartuzumab (black). (A) Saturation binding plot. (B) Lindmo plot.[a]

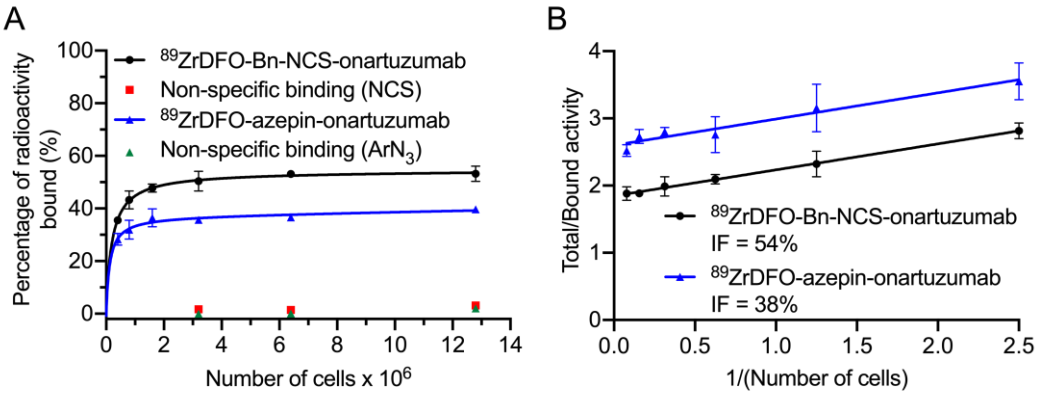

[a] Data account for differences in radiochemical purity.

Animals and xenograft models

All experiments involving mice were conducted in accordance with an animal experimentation licence approved by the Zurich Canton Veterinary Office, Switzerland (Jason P. Holland). Experimental procedures also complied with guidelines issued in the *Guide for the Care and Use of Laboratory Animals.*(*8*) Female athymic nude mice (Crl:NU(NCr)-*Foxn1*^{nu}, 20 – 25 g, 4 – 8 weeks old) were obtained from Charles River Laboratories Inc. (Freiburg im Breisgau, Germany), and were allowed to acclimatise at the University of Zurich Laboratory of Animal Science vivarium for at least 1 week prior to implanting tumour cells. Mice were provided with food and water *ad libitum*. Tumours were induced on the right shoulder or flank by sub-cutaneous (s.c.) injection of approx. 2.5 × 10^6 cells. The cells were injected in a 200 µL suspension of a 1:1 v/v mixture of PBS and reconstituted basement membrane (Corning® Matrigel® Basement Membrane Matrix, obtained from VWR International).(*9*) Tumours developed after a period of between 7 – 14 days. Tumour volume (V / mm^3) was estimated by external Vernier calliper measurements of the longest axis, a / mm, and the axis perpendicular to the longest axis, b / mm. The tumours were assumed to be spheroidal and the volume was calculated in accordance with Equation S1.

$$V = \frac{4\pi}{3} \cdot \left(\frac{a}{2}\right)^2 \cdot \left(\frac{b}{2}\right) \quad \text{(Equation S1)}$$

Small-animal PET imaging

All mice injected with cancer cells developed tumours and the average volume of the MKN-45 tumours was 577 ± 424 mm^3 (*n* = 12 mice; volume range = 135 – 1323 mm^3). Mice were randomised before the study. The tail of each mouse was warmed gently using a warm water bath immediately before administering [^{89}Zr]ZrDFO-azepin-onartuzumab (normal group *n* = 4 mice / group, where each dose contained activity = 0.471 ± 0.047 MBq, equivalent to 30.3 ± 0.31 μg of protein, 0.336 ± 0.031 nmol of protein, in 222 ± 15 μL sterile PBS) *via* intravenous (i.v.) tail-vein injection (*t* = 0 h). Competitive inhibition studies were also performed to investigate the specificity and biological activity of the radiotracer *in vivo* (blocking group: *n* = 4 mice / group, where each dose contained activity = 0.433 ± 0.011 MBq, equivalent to 971 ± 14 μg of protein, 9.79 ± 0.144 nmol of protein, in 208 ± 3 μL sterile PBS). For comparison with standard conjugation and radiolabelling chemistry, PET imaging was also performed on a group of mice administered with [^{89}Zr]ZrDFO-Bn-NCS-onartuzumab (normal group *n* = 4 mice / group, where each dose contained activity 0.571 ± 0.016 MBq, equivalent to 4.04 ± 0.15 μg of protein, 0.041 ± 0.001 nmol of protein, in 210 ± 2 μL sterile PBS). Full details on radioactive dose preparation are given in the Radiochemistry section above.

PET imaging experiments were conducted on a Genesis G4 PET/X-ray scanner (Sofie Biosciences, Culver City, CA).(*10*) Approximately 5 minutes prior to recording each PET image, mice were anesthetised by inhalation of between 2 – 4% isoflurane (Attane™, Piramal Enterprises Ltd, India, supplied by Provet AG, Lyssach, Switzerland)/oxygen gas mixture and placed on the scanner bed in the prone position. PET images were recorded at various time-points between 0 h and 72 h post-administration of the radiotracer. During image acquisition, the respiration rate of the animal was monitored *via* live video feed and anaesthesia was maintained by an experience animal experimenter by controlling the isoflurane dose between 1.5 – 2.0%. List-mode data were acquired for 10 min. using a γ-ray energy window of 150–650 keV, and a

coincidence timing window of 20 ns. Images were reconstructed by iterative ordered subset maximum expectation (OSEM; 60 iterations) protocols. The reported reconstructed spatial resolution is 2.4 μL at the centre of the field-of-view (FOV). Image data were normalised to correct for non-uniformity of response of the PET, attenuation, random events, dead-time count losses, positron branching ratio, and physical decay to the time of injection, but no scatter or partial-volume averaging correction was applied. An empirically determined system calibration factor (in units of [Bq/voxel]/[MBq/g] or [Bq/cm^3]/[MBq/g]) for mice was used to convert voxel count rates to activity concentrations. The resulting image data were normalised to the administered activity to parameterise images in terms of %ID cm^{-3} (equivalent to units of %ID/g assuming a tissue density of unity). Images were analysed by using VivoQuant™ 3.5 patch 2 software (InviCRO, Boston, MA). For image quantification and measurements of time-activity curves (TACs), 3-dimensional volumes-of-interest (VOIs) were drawn manually to determine the maximum and mean accumulation of radioactivity (in units of %ID cm^{-3} and decay corrected to the time of injection) in various tissues. Where appropriate, data were also converted into mean standardised uptake values (SUV_{mean}).

Biodistribution studies

Biodistribution studies were conducted after the final imaging time point to evaluate the radiotracer uptake in tumour-bearing mice. Animals (n = 4 mice / group) were anaesthetised individually by isoflurane and euthanised by isoflurane asphyxiation followed by terminal exsanguination. Note: one mouse was excluded from the analysis of the data from the normal group (*vide supra*). A total of 15 tissues (including the tumour) were removed, rinsed in water, dried in air for approx. 2 min., weighed and counted on a calibrated gamma counter for accumulation of activity. The mass of radiotracer formulation injected into each animal was measured and used to determine the total number of counts per minute (cpm) injected into each mouse by comparison to a standard syringe of known activity and mass. Count data were background- and decay-corrected, and the tissue uptake for each sample (determined in units of percentage injected dose per gram [%ID g^{-1}]) was calculated by normalisation to the total amount of activity injected for each individual animal. For comparison purposes, data are also presented in terms of SUV.

Effective half-life, $t_{1/2}$(eff)

The effective half-lives $t_{1/2}$(eff) of [^{89}Zr]ZrDFO-azepin-onartuzumab and [^{89}Zr]ZrDFO-Bn-NCS-onartuzumab were measured in the same athymic nude mice used for small-animal PET imaging and end time point biodistribution. Total internal radioactivity was measured as a function of time by using a dose calibrator.

Statistical analysis

Where appropriate, data were analysed by the unpaired, two-tailed Student's *t*-test. Differences at the 95% confidence level (*P*-value <0.05) were considered to be statistically significant. Data analysis was performed using Microsoft Excel for MAC (version 16.16.10) and GraphPad Prism 7 for MAC OS X (version 7.0e).

PET imaging results

Supplemental Figure 5. Temporal PET images recorded in athymic nude mice bearing MKN-45 tumours on the right flank at time points between 0 h to 72 post-administration of (top) [^{89}Zr]ZrDFO-Bn-NCS-onartuzumab, (middle) [^{89}Zr]ZrDFO-azepin-onartuzumab (normal group), and (bottom) [^{89}Zr]ZrDFO-azepin-onartuzumab (blocking group). T = tumour, H = heart, L = liver, Sp = spleen. Coronal and axial planes are through the tumour centre.

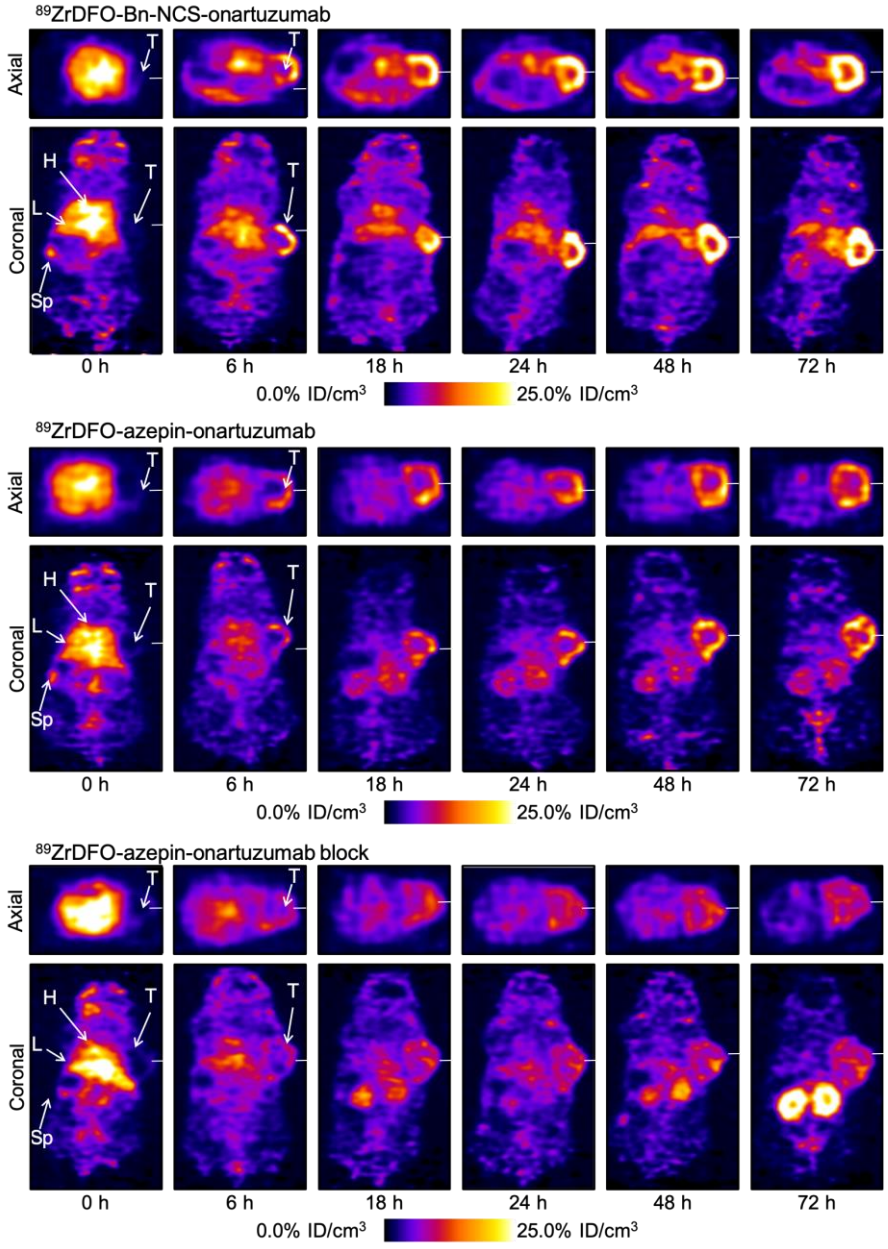

Supplemental Figure 6. Maximum intensity projection (MIP) PET images recorded in athymic nude mice bearing MKN-45 tumours on the right flank at time points between 0 h to 72 post-administration of (top) [^{89}Zr]ZrDFO-Bn-NCS-onartuzumab, (middle) [^{89}Zr]ZrDFO-azepin-onartuzumab (normal group), and (bottom) [^{89}Zr]ZrDFO-azepin-onartuzumab (blocking group). T = tumour, H = heart, L = liver, Sp = spleen, B = bladder, K = kidney.

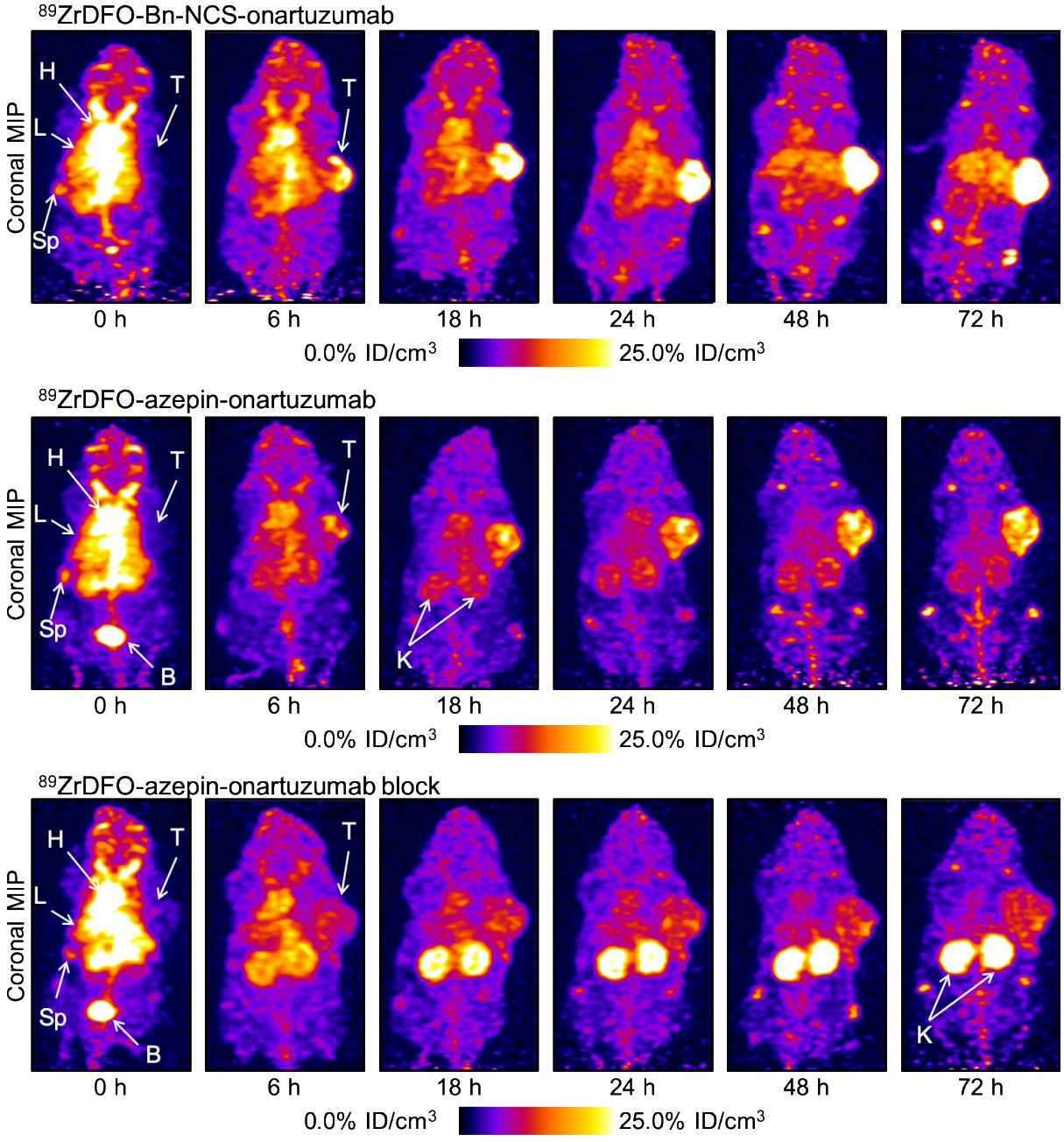

Supplemental Figure 7. Time-activity bar chart showing the activity associated with different tissues (volumes-of-interest, VOI) *versus* time (from 0 to 72 h post-administration). Data presented are based on quantification of the PET images (in units of %ID cm^{-1}) for [^{89}Zr]ZrDFO-Bn-NCS-onartuzumab (blue bars), [^{89}Zr]ZrDFO-azepin-onartuzumab (normal group; red-to-yellow bars), and [^{89}Zr]ZrDFO-azepin-onartuzumab (blocking group; black-to-white bars).

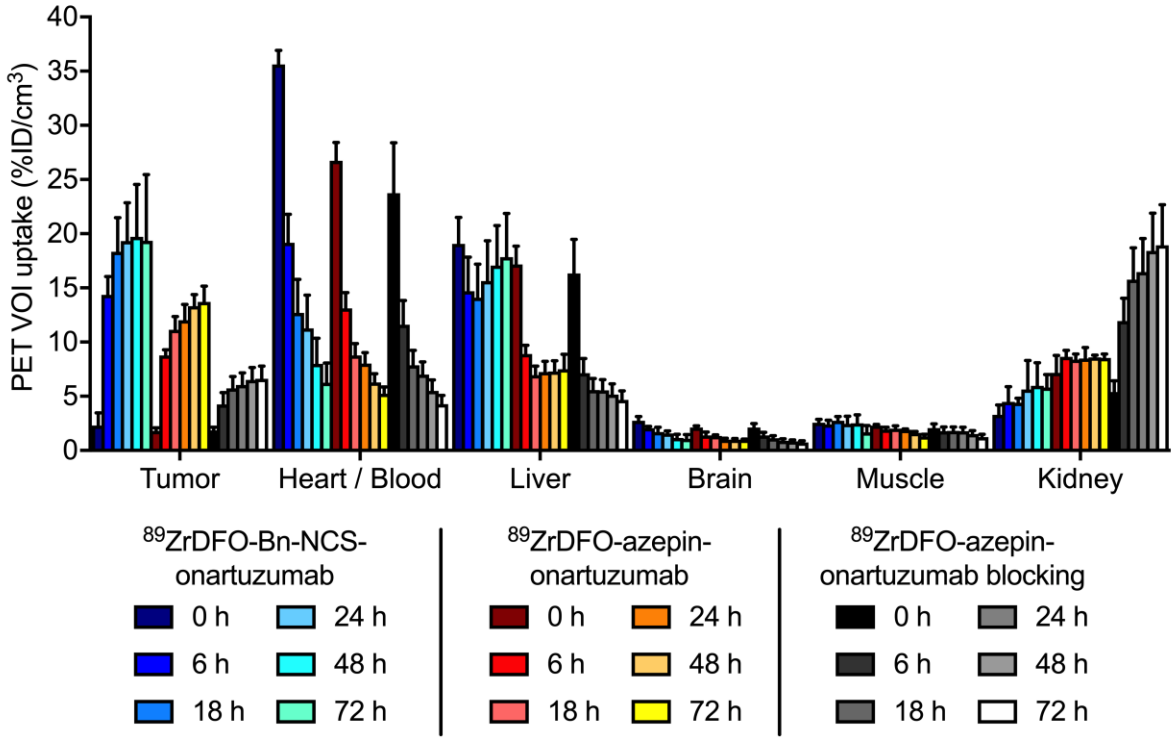

Supplemental Figure 8. Plot of the measured activity retained in each mouse *versus* time.[a] Data were used to estimate the effective and biological half-lives of [^{89}Zr]ZrDFO-Bn-NCS-onartuzumab and [^{89}Zr]ZrDFO-azepin-onartuzumab.

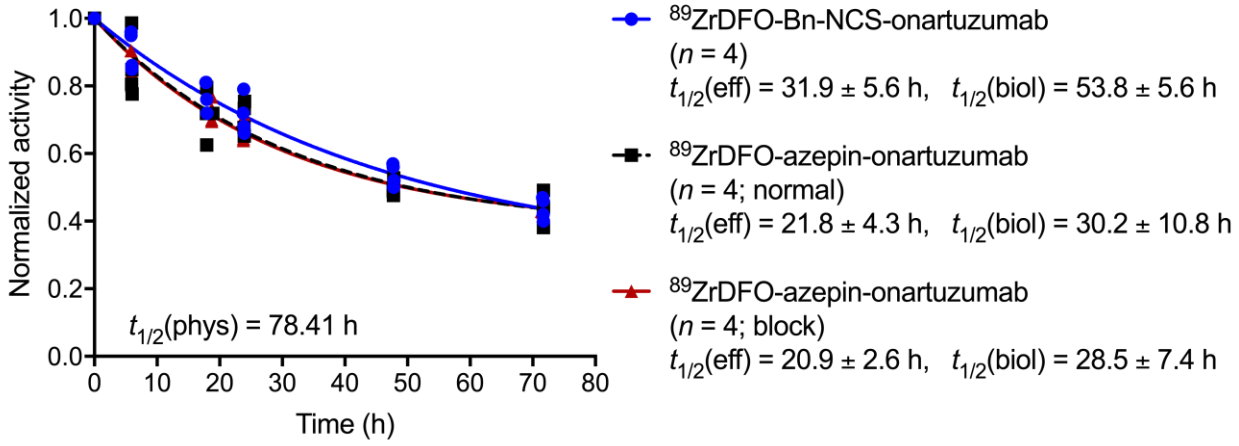

[a] Data account for differences in radiochemical purity.

Biodistribution data

Supplemental Figure 9. Bar chart showing *ex vivo* biodistribution data (SUV) for the uptake of [^{89}Zr]ZrDFO-Bn-NCS-onartuzumab (blue bars), [^{89}Zr]ZrDFO-azepin-onartuzumab (normal group, white bars), and [^{89}Zr]ZrDFO-azepin-onartuzumab (blocking group, red bars) in mice bearing MKN-45 tumours. Data were recorded after the final imaging time point at 72 h post-injection. Student's *t*-test: (ns) not significant, (*) *P*-value < 0.05, (**) *P*-value < 0.01, (***) *P*-value < 0.001.

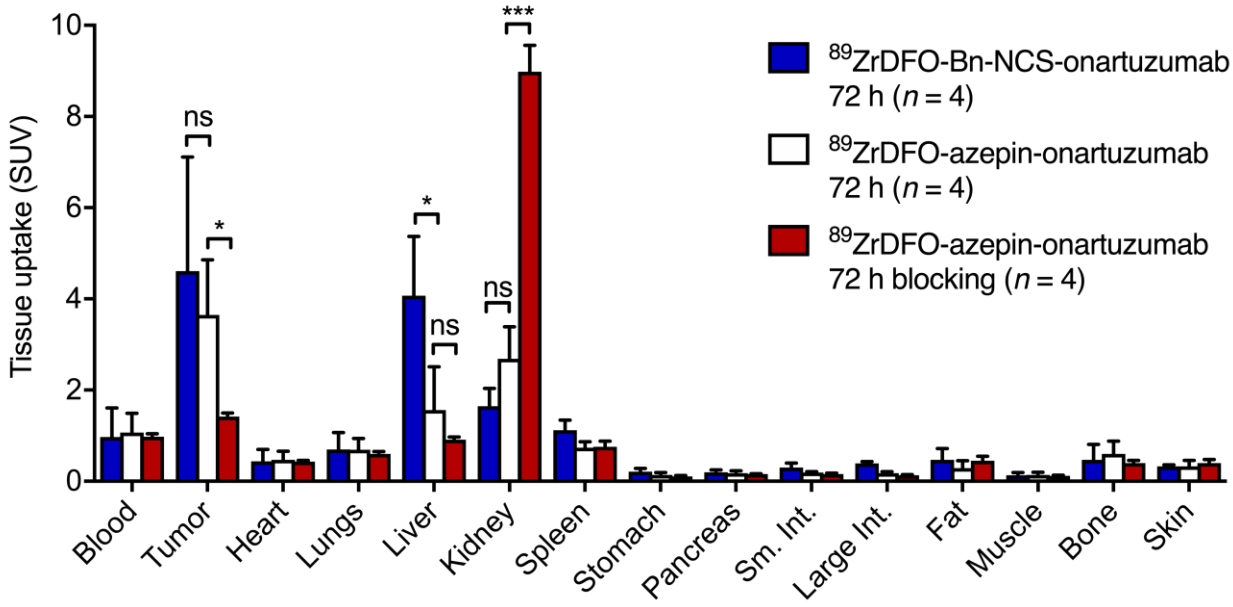

Supplemental Figure 10. Bar chart showing tumour-to-tissue contrast ratio calculated from the *ex vivo* biodistribution data (recorded at 72 h post-administration in units of %ID g^{-1}) for the uptake of [^{89}Zr]ZrDFO-Bn-NCS-onartuzumab (blue bars), [^{89}Zr]ZrDFO-azepin-onartuzumab (normal group, white bars), and [^{89}Zr]ZrDFO-azepin-onartuzumab (blocking group, red bars) in mice bearing MKN-45 tumours.

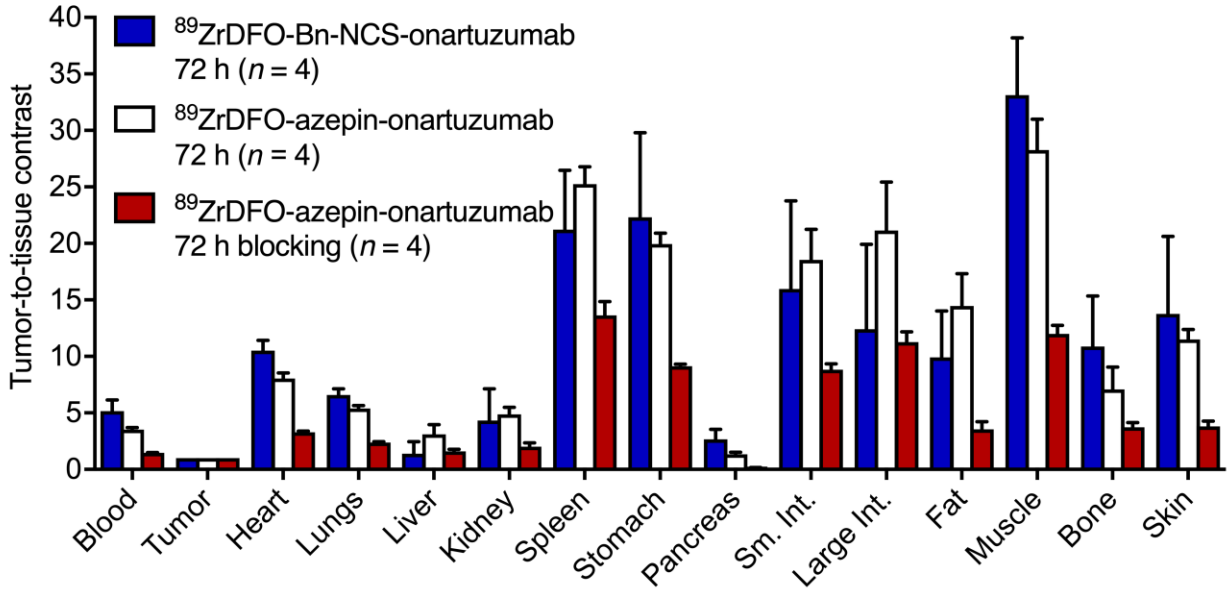

Supplemental Table 2. Ex vivo biodistribution data measured at 72 h after i.v. administration of ^{89}ZrDFO-azepin-onartuzumab (normal and blocking groups) and ^{89}ZrDFO-Bn-NCS-onartuzumab in female athymic nude mice bearing subcutaneous MKN-45 tumors. [a] Uptake data are expressed as the mean %ID g^{-1} ± one standard deviation (S.D.). [b] Errors for the tumor-to-tissue ratios are calculated as the standard deviations based on ratios from dependent pairs.

	^{89}ZrDFO-azepin-onartuzumab (normal group, *n* = 4)		^{89}ZrDFO-azepin-onartuzumab (blocking group, *n* = 4)		^{89}ZrDFO-Bn-NCS-onartuzumab (control group, *n* = 4)	
Tissue	Uptake / %ID g^{-1} ± S.D.[a]	Tumor-to-tissue contrast ratio ± S.D.[b]	Uptake / %ID g^{-1} ± S.D.[a]	Tumor-to-tissue contrast ratio ± S.D.[b]	Uptake / %ID g^{-1} ± S.D.[a]	Tumor-to-tissue contrast ratio ± S.D.[b]
Blood	4.49 ± 1.79	3.53 ± 0.36	4.35 ± 0.27	1.46 ± 0.08	4.50 ± 2.98	5.15 ± 0.99
Tumor	15.37 ± 5.21	1.00	6.34 ± 0.47	1.00	21.38 ± 11.57	1.00
Heart	1.98 ± 0.83	8.05 ± 0.97	1.92 ± 0.15	3.30 ± 0.18	2.05 ± 1.20	10.52 ± 0.91
Lungs	2.88 ± 1.02	5.39 ± 0.54	2.69 ± 0.36	2.38 ± 0.17	3.23 ± 1.72	6.59 ± 0.55
Liver	6.56 ± 4.03	3.11 ± 1.72	4.12 ± 0.94	1.60 ± 0.36	18.84 ± 6.03	1.38 ± 1.07
Spleen	3.10 ± 0.50	4.87 ± 1.23	3.49 ± 1.42	2.02 ± 0.66	5.22 ± 1.10	4.34 ± 2.79
Stomach	0.61 ± 0.23	25.25 ± 3.07	0.48 ± 0.10	13.63 ± 2.45	0.96 ± 0.33	21.22 ± 5.24
Pancreas	0.76 ± 0.21	19.95 ± 1.93	0.69 ± 0.04	9.13 ± 0.40	0.92 ± 0.25	22.31 ± 7.50
Kidney	11.28 ± 2.62	1.35 ± 0.36	40.05 ± 3.27	0.16 ± 0.01	7.64 ± 1.80	2.66 ± 0.89
Sm. Int.	0.82 ± 0.10	18.55 ± 5.40	0.73 ± 0.11	8.82 ± 1.06	1.38 ± 0.46	15.97 ± 7.79
Large Int.	0.76 ± 0.11	21.15 ± 8.55	0.58 ± 0.12	11.27 ± 1.82	1.79 ± 0.18	12.41 ± 7.50
Fat	1.21 ± 0.68	14.46 ± 5.71	2.06 ± 1.06	3.55 ± 1.37	2.19 ± 1.19	9.92 ± 4.09
Muscle	0.58 ± 0.24	28.26 ± 5.49	0.53 ± 0.03	12.00 ± 1.49	0.62 ± 0.26	33.13 ± 5.06
Bone	2.50 ± 1.08	7.08 ± 3.93	1.75 ± 0.36	3.74 ± 0.81	2.18 ± 1.58	10.88 ± 4.46
Skin	1.40 ± 0.57	11.49 ± 1.79	1.77 ± 0.57	3.80 ± 0.94	1.52 ± 0.13	13.75 ± 6.88

References

1. Patra M, Klingler S, Eichenberger LS, Holland J. Simultaneous Photoradiochemical Labelling of Antibodies for Immuno-PET. *iScience*. 2019;13:416-431.
2. Zanzonico P. Routine Quality Control of Clinical Nuclear Medicine Instrumentation: A Brief Review. *J Nucl Med*. 2008;49:1114-1131.
3. Fay R, Gut M, Holland JP. Photoradiosynthesis of 68Ga-Labeled HBED-CC-Azepin-MetMAb for Immuno-PET of c-MET Receptors. *Bioconjug Chem*. 2019;30:1814-1820.
4. Vosjan MJWD, Perk LR, Visser GWM, et al. Conjugation and radiolabeling of monoclonal antibodies with zirconium-89 for PET imaging using the bifunctional chelate p-isothiocyanatobenzyl-desferrioxamine. *Nat Protoc*. 2010;5:739-743.
5. Perk LR, Vosjan MJWD, Visser GWM, et al. P-Isothiocyanatobenzyl-desferrioxamine: A new bifunctional chelate for facile radiolabeling of monoclonal antibodies with zirconium-89 for immuno-PET imaging. *Eur J Nucl Med Mol Imaging*. 2010;37:250-259.
6. Holland JP, Divilov V, Bander NH, Smith-Jones PM, Larson S, Lewis JS. ^{89} Zr-DFO-J591 for immunoPET of prostate-specific membrane antigen expression in vivo. *J Nucl Med*. 2010;51.
7. Lindmo T, Boven E, Cuttitta F, Fedorko J, Bunn PA. Determination of the immunoreactive function of radiolabeled monoclonal antibodies by linear extrapolation to binding at infinite antigen excess. *J Immunol Methods*. 1984;72:77-89.
8. Institute for Laboratory Animal Research. Guide for the Care and Use of Laboratory Animals: 8th Ed.; 2011.
9. Fridman R, Benton G, Aranoutova I, Kleinman HK, Bonfil RD. Increased initiation and growth of tumor cell lines, cancer stem cells and biopsy material in mice using basement membrane matrix protein (Cultrex or Matrigel) co-injection. *Nat Protoc*. 2012;7:1138-1144.
10. Bai B, Dahlbom M, Park R, et al. Performance comparison of GENISYS4 and microPET preclinical PET scanners. *IEEE Nucl Sci Symp Conf Rec*. 2012;bai:3765-3768.